Pharm Res (2015) 32:211–221
DOI 10.1007/s11095-014-1456-6

RESEARCH PAPER

Oxidative Stress Protection by Exogenous Delivery of rhHsp70 Chaperone to the Retinal Pigment Epithelium (RPE), a Possible Therapeutic Strategy Against RPE Degeneration

Astrid Subrizi • Elisa Toropainen • Eva Ramsay • Anu J. Airaksinen • Kai Kaarniranta • Arto Urtti

Received: 24 March 2014 / Accepted: 2 July 2014 / Published online: 17 July 2014

ABSTRACT

Purpose To measure the cytoprotective effects of rhHsp70 against oxidative stress and study its cellular uptake, intracellular and intraocular distribution in the retinal pigment epithelium.

Methods Human retinal pigment epithelial cells (ARPE-19) were pre-treated with rhHsp70 for 24 h, 48 h, and 72 h before being exposed to 1.25 mM hydrogen peroxide. Non-treated cells served as control. We analysed interleukin 6 secretion, cell viability, and cytolysis. Uptake and intracellular distribution of fluorescently labelled rhHsp70 were investigated with flow cytometry and confocal microscopy, respectively. Ocular distribution of radioactively labelled rhHsp70 was followed *ex vivo* in porcine eyes by micro SPECT/CT.

Results After exposure to hydrogen peroxide, IL-6 secretion decreased by 35–39% when ARPE-19 cells were pre-treated with rhHsp70. Cell viability increased by 17–32%, and cell lysis, measured by the release of lactate dehydrogenase, decreased by 6-43%. ARPE-19 cells endocytosed rhHsp70 added to the culture medium and the protein was localized in late endosomes and lysosomes. Following intravitreal injection into isolated porcine eyes, we found 20% rhHsp70 in the RPE.

Conclusions Recombinant hHsp70 protein offers protection against oxidative stress. RPE cells take up the exogenously delivered rhHsp70 and localize it in late endosomes and lysosomes. This work provides the basis for a therapeutic strategy to target aggregate-associated neurodegeneration in AMD.

KEY WORDS AMD · Hsp70 · Oxidative stress · Protein delivery · RPE

Subrizi and Toropainen have contributed equally to this work

Electronic supplementary material The online version of this article (doi:10.1007/s11095-014-1456-6) contains supplementary material, which is available to authorized users.

A. Subrizi (✉) · E. Ramsay · A. Urtti
Centre for Drug Research, Division of Pharmaceutical Biosciences
Faculty of Pharmacy, University of Helsinki, Helsinki, Finland
e-mail: astrid.subrizi@helsinki.fi

E. Toropainen · K. Kaarniranta
Department of Ophthalmology, Institute of Clinical Medicine
University of Eastern Finland, Kuopio, Finland

A. J. Airaksinen
Laboratory of Radiochemistry, Department of Chemistry
University of Helsinki, Helsinki, Finland

K. Kaarniranta
Department of Ophthalmology, Kuopio University Hospital
Kuopio, Finland

A. Urtti
School of Pharmacy, University of Eastern Finland Kuopio
Finland

ABBREVIATIONS

AMD	Age-related macular degeneration
Hsp	Heat shock protein
ROS	Reactive oxygen species
RPE	Retinal pigment epithelium

INTRODUCTION

Age-related macular degeneration (AMD) is a progressive, neurodegenerative ocular disease and leading cause of blindness in the elderly in developed countries. Age-related changes predisposing a person to AMD occur in the outer retina that includes the photoreceptors, the retinal pigment epithelium (RPE), and Bruch's membrane (1). Due to its essential functions of maintenance and homeostasis, the RPE is particularly important for retinal health: RPE dysfunction and degeneration are critical events in AMD pathogenesis. During a person's lifetime, RPE cells endure high levels of oxidative stress because of their substantial consumption of oxygen,

accumulation of lipid peroxidation products from ingested photoreceptor outer segments, and constant exposure to light (2, 3). In healthy RPE cells, however, this harmful and potentially damaging microenvironment is neutralized by the presence of a range of antioxidant and efficient repair systems. Unfortunately, as we age oxidative damage caused by reactive oxygen species (ROS) increases, antioxidant capacity decreases and the efficiency of reparative systems becomes impaired (4). ROS such as singlet oxygen, superoxide and hydrogen peroxide, are highly reactive and toxic molecules that can lead to lipid, protein, and DNA damage, as well as mitochondrial dysfunction. Oxidative stress in the retina is further aggravated by growing amounts of lipofuscin, the autofluorescent age-pigments consisting of photo-sensitive bisretinoid compounds that can generate ROS, in the lysosomes of RPE cells, especially in AMD eyes (5). Chronic exposure to oxidative stress and a decline in lysosomal activity may eventually lead to the aberrant folding, aggregation, and accumulation of proteins resulting in cellular damage and tissue dysfunction. Virtually all cells respond to these potentially toxic conditions by induction of a set of highly conserved genes that encode heat shock proteins (Hsps). This set of proteins functions as the major cellular defense against the accumulation of damaged or mutant proteins (6, 7). Hsps, together with cellular clearance mechanisms such as the ubiquitin proteasome system and autophagy, are responsible for protein quality control (8), hence fulfilling a key role in the proteostasis network. The essential tasks of Hsps include assisting in the refolding of damaged proteins, facilitating their translocation to their correct intracellular localization, and mitigating the harmful effects of protein misfolding and aggregation (9). Several studies indicate that weakening of the heat shock response is a common effect in aging cells that has been observed in various tissues (10–17), as well as in the RPE of human donor AMD eyes, where recent studies (18–20) found decreased expression of Hsps, including Hsp70, lysosomal Hsc70, mitochondrial mtHsp70, Hsp60, and αA crystallin. The senescent RPE seems to fail to induce an appropriate heat shock reaction in response to oxidative damage. In contrast to the aging RPE, the human retinal pigment epithelium cell line ARPE-19 upregulated the expression of Hsp27, Hsp40, and Hsp70 after oxidant-mediated injury (21–24). Furthermore, an increase in Hsp expression correlated with cell differentiation and enhanced resistance to oxidative stress (25, 26). Our previous work has shown that Hsp70 participates in the clearance of aggregates induced by the inhibition of the proteasome in ARPE-19 cells (8). However, when ARPE-19 cells were cultured on advanced glycation end products (AGE)-modified basement membrane, the expression of Hsps was significantly down regulated (27).

Given the ability of non-senescent RPE cells to effectively tackle oxidative stress and clear lysosomal aggregates, we hypothesize that exogenous delivery of rhHsp70 may provide a therapeutic strategy to target aggregate-associated neurodegeneration in AMD. Here we study the cytoprotective properties of rhHsp70 against oxidative damage and the feasibility of rhHsp70 protein therapy. Our study demonstrates that rhHsp70 treatment protects ARPE-19 cells from oxidative harm by reducing inflammation, increasing cell viability and decreasing cytolysis. We also establish that exogenously delivered rhHsp70 is internalized by dividing and differentiated ARPE-19 cells and is subsequently localized in late endosomes and lysosomes. Moreover, preliminary experiments with isolated porcine eyes indicate that rhHsp70 is able to reach the retina after intravitreal injection. Together our results provide a rationale for future testing of a prolonged action rhHsp70 protein therapy to mitigate damage of the RPE.

MATERIALS AND METHODS

Materials

Recombinant human Hsp70 (rhHsp70, 72 kDa) was from Enzo Life Sciences (Farmingdale, NY, USA). Labeling reagents: Alexa Fluor 488 microscale protein labeling kit was from Molecular Probes (Thermo Fisher Scientific, Waltham, MA, USA), sodium iodide ^{123}I labeling solution in 0.1 M sodium hydroxide was from MAP Medical Technologies (Helsinki, Finland), Pierce pre-coated iodination tubes (12 x 75 mm coated with 50 μg Pierce iodination reagent) were from Thermo Fisher Scientific (Waltham, MA, USA), Sephadex PD MiniTrap G-25 columns were from GE Healthcare Bio-Sciences (Uppsala, Sweden). Cell culture reagents were from Life Technologies (Thermo Fisher Scientific, Waltham, MA, USA), except for mouse laminin from BD Biosciences (San Jose, CA, USA). Hydrogen peroxide was from Sigma-Aldrich (St. Louis, MO, USA), the human IL-6 ELISA OptEIATM kit was from BD Pharmingen (San Jose, CA, USA), MTT was from Sigma-Aldrich (St. Louis, MO, USA), CytoTox 96 nonradioactive cytotoxicity assay kit was from Promega (Madison, WI, USA), CellLight Late Endosomes-RFP and CellLight Lysosomes-RFP were from Molecular Probes (Thermo Fisher Scientific, Waltham, MA, USA).

rhHsp70 Protein Labeling

Recombinant human Hsp70 protein was labeled with Alexa Fluor 488 tetrafluorophenyl reactive dye using the microscale protein labeling kit and following the manufacturer's instructions. The labeled protein was separated from the unreacted dye with spin filters, also provided with the kit. The conjugates were analyzed using a SPECTROstar Nano spectrometer (BMG Labtech, Ortenberg, Germany), aliquoted and stored at −80°C until further use.

Recombinant human Hsp70 protein was radio-iodinated following the Iodo-Gen method. Briefly, 10 μg rhHsp70 were diluted in 50 μl sodium phosphate buffer (0.2 M, pH 7.4), then combined with 100 MBq $Na^{123}I$ labeling solution in a Iodo-Gen pre-coated tube. After 15 min reaction time with occasional mixing, the mixture was transferred to a tube containing 250 μl tyrosine solution (50 μg/ml) to stop the iodination reaction. The radiolabeled protein was separated from the remaining radioactive iodide and radiolabeled tyrosine by gel filtration with Sephadex PD MiniTrap G-25 columns using sodium phosphate buffer (0.2 M, pH 7.4) as eluting buffer. Purified [^{123}I] rhHsp70 was analyzed on Whatman 1 chromatography paper (Millipore, Billerica, MA, USA) using a mixture of methanol and water (50:50) as eluent (R_f [^{123}I]rhHsp70 = 0.0, R_f [^{123}I] tyrosine and $Na^{123}I$ = 1.0). The chromatography paper was exposed to digital imaging plate (Fujifilm Corporation, Japan), scanned on a Fujifilm FLA-5100 scanner and analyzed with AIDA 2.0 imaging software (Raytest Isotopenmessgeräte GmbH, Germany). Radioiodinated rhHsp70 protein was used immediately after labeling.

Cell Culture

ARPE-19 cells (human retinal pigment epithelial cell line, ATCC CRL-2302) were cultured in Dulbecco's Modified Eagle Medium:Nutrient Mixture F-12 (DMEM/F-12) supplemented with 10% fetal bovine serum (FBS), 2 mM L-glutamine and antibiotics. The cells were subcultured once a week. For filter culture, cells were seeded at a density of 1.6×10^5 cells/cm^2 on laminin coated Transwell permeable supports (surface area 4.67 cm^2, pore size 0.4 μm, Corning Life Sciences, Corning, NY, USA) and differentiated for 4 weeks (for details see (28)). The culture medium of filter grown ARPE-19 cells contained only 1% FBS, but was otherwise same as above. The cells were maintained at 37°C in 5 or 7% CO_2.

rhHsp70 Protein Treatment

ARPE-19 cells were seeded on 24-well plates at a density of 100,000 cells/well. The cells were differentiated for four weeks and then divided into four groups: control group (no treatment), rhHsp70 group (protein treatment), rhHsp70/H_2O_2 group (protein treatment followed by exposure to oxidative stress), and H_2O_2 group (exposure to oxidative stress). At first, groups rhHsp70 and rhHsp70/H_2O_2 were treated with recombinant human Hsp70 protein at a concentration of 5 μg/ml. After 24 h, 48 h, or 72 h the cell culture medium was replaced and groups rhHsp70/H_2O_2 and H_2O_2 were exposed to1.25 mM hydrogen peroxide. The exposure to H_2O_2 was repeated after 24 h (total exposure time: 48 h).

IL-6 Secretion

IL-6 is a pro-inflammatory cytokine, whose release increases in response to inflammation and cell/tissue injury. The concentration of IL-6 (pg/ml) in the cell culture medium was measured by a commercial enzyme-linked immunosorbent assay (ELISA) using OptEIATM sets. The method was performed according to the manufacturer's instructions. Absorbance was measured at a wavelength of 450 nm with a reference wavelength of 655 nm using a plate reader (Bio-Rad Model 550, Bio-Rad, Hercules, CA, USA).

MTT Assay

Cell viability was analyzed by MTT assay. In this method, NAD (P) H-dependent cellular oxidoreductase enzymes reduce the tetrazolium dye MTT 3-(4,5-dimethylthiazol-2-yl)-2,5-diphenyltetrazolium bromide to insoluble formazan in the mitochondria of living cells. The assay was performed as previously described (29). The absorbance was measured at a wavelength of 595 nm using a plate reader (Bio-Rad Model 550, Bio-Rad, Hercules, CA, USA). The cell viability was presented as percentage of the control group.

LDH Release

Lactate dehydrogenase (LDH) is released into the cell culture medium after cell membrane damage. LDH was detected by CytoTox 96 nonradioactive cytotoxicity assay kit according to the manufacturer's instructions. LDH activity was quantified using a plate reader (Bio-Rad Model 550, Bio-Rad, Hercules, CA, USA) with a measurement wavelength of 490 nm and reference wavelength of 655 nm.

rhHsp70 Cell Uptake

Dividing ARPE-19 cells were seeded on 6-well plates at a density of 500,000 cells/well one day before the uptake experiment. Differentiated ARPE-19 cells were used after 4 weeks differentiation on filter. On the experiment day, cells were washed with HBSS buffer supplemented with 10 mM Hepes (pH 7.4) and then equilibrated in the same buffer for 30 min in the cell incubator. The cells were incubated with Alexa Fluor 488-labeled rhHsp70 (0.26 μg/cm^2) for 1 h, at 37°C. Subsequently the cells were rinsed with buffer, detached from the wells with trypsin (0.05 g/l)-EDTA (0.02 g/l), diluted with buffer and centrifuged at 1200 rpm for 5 min. After discarding most of the supernatant, the cells were gently re-suspended in buffer and immediately analyzed by flow cytometry (LSR II, BD Biosciences, San Jose, CA, USA) with a blue solid-state laser (488 nm) as the excitation source. Fluorescence of labeled rhHsp70 was collected with a 530/30 band-pass filter. For each sample 10,000 events were

collected. Control cells were visualized on a forward angle light scatter (FSC) *versus* a 90° angle side scatter (SSC) display. The major cell population was gated and only cells falling within this area were used for further analysis. Data collection was controlled using FACSDiva software (BD Biosciences, San Jose, CA, USA) and data analysis was performed with FlowJo software (Tree Star, Ashland, OR, USA). The Overton cumulative histogram subtraction algorithm was used to calculate the percentage of positive cells.

rhHsp70 Intracellular Distribution

Dividing ARPE-19 cells were seeded on Nunc Lab-Tek II chambered cover glass (1.7 cm^2) (Thermo Fisher Scientific, Waltham, MA, USA) at a density of 50,000 cells/well two days before the uptake experiment. Differentiated ARPE-19 cells were used after 4 weeks differentiation on Lab-Tek II chambered cover glass (1.7 cm^2). The next day, lysosomes or late endosomes were stained with CellLight Lysosomes/Late endosomes-RFP reagent following the manufacturer's instructions and the cells were returned to the incubator for 16 h. On the experiment day, the cells were incubated with Alexa Fluor 488-labeled rhHsp70 (0.6 μg/cm^2) for 1 h, at 37°C. Subsequently the cells were rinsed with cell culture medium, and immediately imaged with an inverted spinning disk confocal microscope (Marianas, 3i Intelligent Imaging Innovations, Ringsby, CT, USA) equipped with a temperature control system and a CO_2 chamber. The cells were observed using a 63x/1.2 W C-Apochromat Corr WD= 0.28 M27 objective, a blue (488 nm/50 mW), and a lime (561 nm/50 mW) solid state lasers. 3D multichannel image processing was performed using Imaris software (Bitplane AG, Zurich, Switzerland).

rhHsp70 Intraocular Distribution

Fresh porcine eyes were obtained from a slaughterhouse (HK Ruokatalo, Forssa, Finland) one day before the experiment and kept at +4°C in a balanced salt solution (BSS Plus, Alcon Laboratories, Forth Worth, TX, USA). On the experiment day, extraocular tissues were removed and the eyes were quickly dipped in 70% ethanol before injection of 100 μl [^{123}I] rhHsp70 (about 4 MBq) with a Micro-Fine 30 gauge needle (0.30 mm x 8 mm, Terumo, Japan). The injection site was located 3–4 mm behind the limbus and the needle was directed towards the center of the vitreous. The eyes were imaged with a NanoSPECT/CT (Mediso, Budapest, Hungary) at 30 min, 2 h, 4 h, and 24 h post-injection in 20 projections using a time per projection of 120 s (for 30 min, 2 h, and 4 h) and 150 s/250 s (for 24 h). CT imaging was carried out with a 45 kVp tube voltage in 240 projections. SPECT images were reconstructed with HiSPECT NG software (Scivis, Göttingen, Germany) and fused with CT datasets using InVivoScope software (Bioscan, Poway, CA, USA). The eyes were kept at 37°C in BSS Plus when they were not imaged. After the last time point (24 h) the vitreous, retina, RPE, and sclera were collected, weighted and their radioactivity measured with a gamma counter (Wallac 1480 Wizard 3", Turku, Finland).

STATISTICAL ANALYSIS

Mann–Whitney *U*-test was used to study the statistical significance of the results in the IL-6 secretion, MTT, and LDH release assays. The significance level of the test was set to 0.05.

RESULTS

Labeling of rhHsp70

The degree of labeling (DOL) of the Alexa Fluor 488 dye-labeled rhHsp70 protein was analyzed with a spectrometer and we obtained a DOL of 5.68. The DOL is a measure of the labeling efficiency and indicates the average number of dye molecules attached to the protein. The radio-iodination reaction had a radiochemical yield of 31.3% and the radiochemical purity of the injected [^{123}I] rhHsp70 was 95.9%.

rhHsp70 Protects ARPE-19 Cells from Oxidative Damage

Pre-treatment with rhHsp70 (rhHsp70/H_2O_2) prior to the exposure of ARPE-19 cells to oxidative stress decreased IL-6 release by 39% (24 h treatment), 36% (48 h treatment), and 35% (72 h treatment) compared to cells that were not treated (H_2O_2) (Fig. 1). The results were statistically significant (P= 0.008 for 24 h treatment, P=0.019 for 48 h treatment, and P=0.038 for 72 h treatment). Addition of rhHsp70 (5 μg/ml) to ARPE-19 did not increase the release of IL-6 compared to control cells (P=0.422, 0.208, and 0.737 respectively).

Pre-treatment with rhHsp70 (rhHsp70/H_2O_2) prior to the exposure of ARPE-19 cells to oxidative stress increased cell viability by 17% (24 h treatment), 32% (48 h treatment), and 29% (72 h treatment) compared to cells that were not treated (H_2O_2) (Fig. 2). The results were statistically significant (P=0.036 for 24 h treatment, P<0.001 for 48 h treatment, and P=0.035 for 72 h treatment). Also, for the 24 h treatment, there was no statistical difference between control cells and rhHsp70 pre-treated cells (rhHsp70/H_2O_2) (P=0.075).

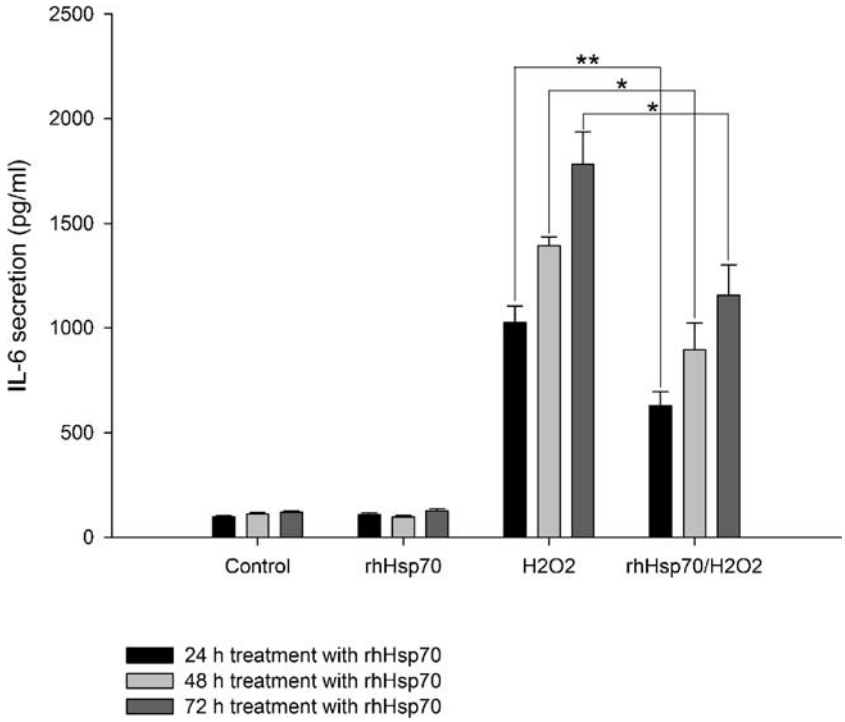

Fig. 1 IL-6 secretion in ARPE-19 cells after exposure to 1.25 mM H_2O_2. Cells were pre-treated with 5 μg/ml rhHsp70 for 24 h,48 h, or 72 h before the oxidative challenge. IL-6 concentration in the culture medium was measured with a commercial ELISA assay. Absorbance was measured at 450 nm with a reference wavelength of 655 nm. According to Mann–Whitney *U*-test, treatment with rhHsp70, prior to the exposure to H_2O_2, decreased IL-6 release in ARPE-19 cells. Statistical significance: * = $P < 0.05$, ** = $P < 0.01$, and *** = $P < 0.001$. Data are presented as mean + S.E.M., $n = 4$.

Pre-treatment with rhHsp70 (rhHsp70/H_2O_2) prior to the exposure of ARPE-19 cells to oxidative stress decreased cytolysis by 43% (24 h treatment), 33% (48 h treatment), and 6% (72 h treatment) compared to cells that were not treated (H_2O_2) (Fig. 3). The results were statistically significant (P= 0.035 for 24 h treatment, P=0.041 for 48 h treatment, and P=0.020 for 72 h treatment). Addition of rhHsp70 (5 µg/ml) to ARPE-19 cells was not cytotoxic.

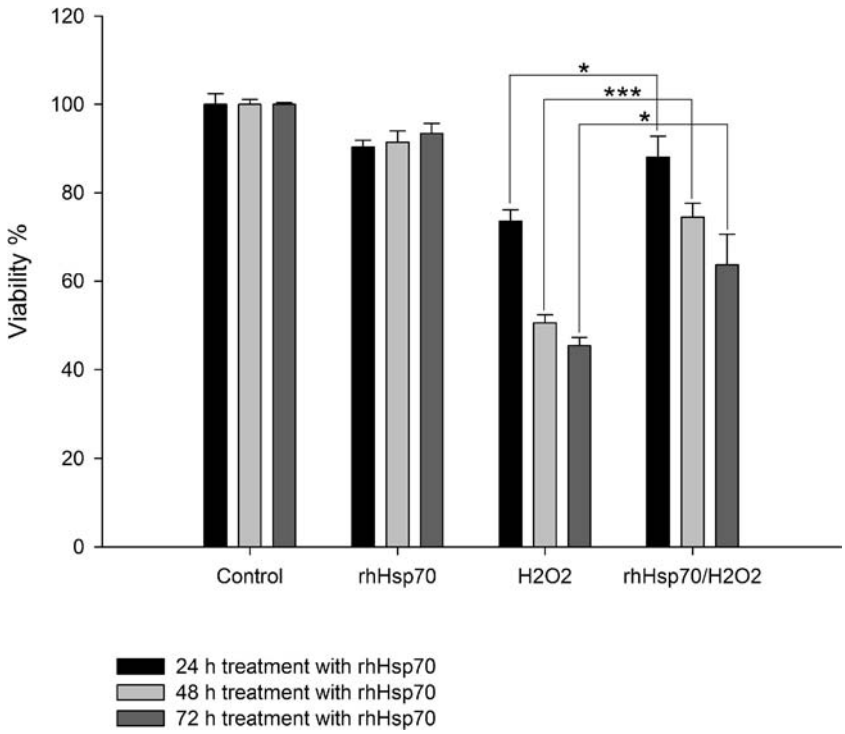

Fig. 2 Viability of ARPE-19 cells after exposure to 1.25 mM H_2O_2. Cells were pre-treated with 5 μg/ml rhHsp70 for 24 h, 48 h, or 72 h before the oxidative challenge. Cell viability was evaluated by MTT assay. Absorbance was measured at 595 nm. According to Mann–Whitney *U*-test, treatment with rhHsp70, prior to the exposure to H_2O_2, increased cell viability of ARPE-19 cells. Statistical significance: * = $P < 0.05$, ** = $P < 0.01$, and *** = $P < 0.001$. Data are presented as mean + S.E.M., n = 4.

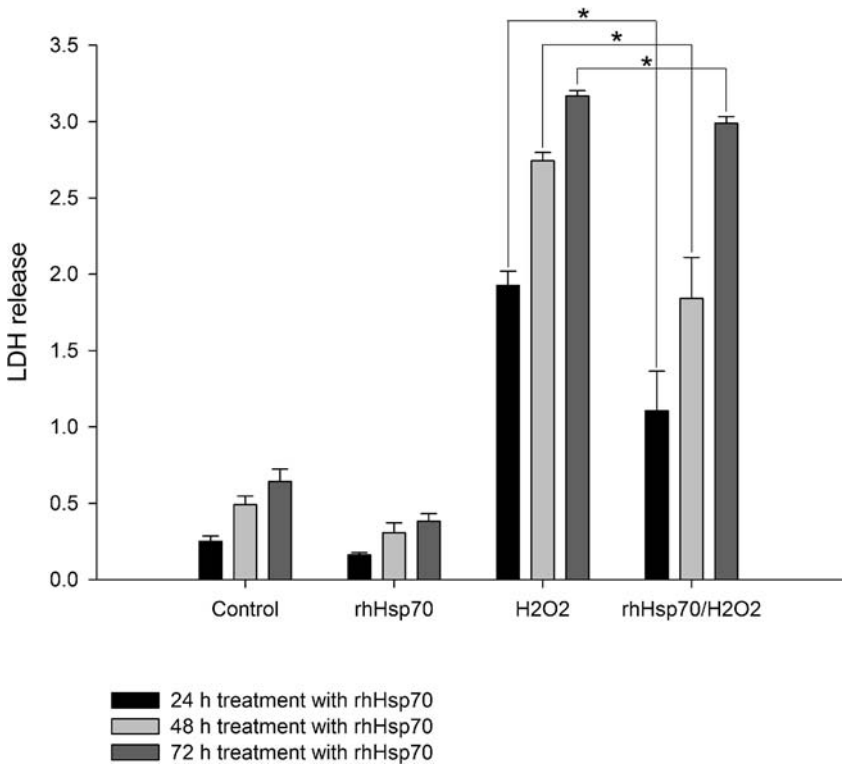

Fig. 3 LDH release in ARPE-19 cells after exposure to 1.25 mM H_2O_2. Cells were pre-treated with 5 μg/ml rhHsp70 for 24 h, 48 h, or 72 h before the oxidative challenge. LDH was detected by CytoTox 96 nonradioactive cytotoxicity assay kit with a measurement wavelength of 490 nm and reference wavelength of 655 nm. According to Mann–Whitney *U*-test, treatment with rhHsp70, prior to the exposure to H_2O_2, decreased cytolysis of ARPE-19 cells. Statistical significance: * = $P < 0.05$, ** = $P < 0.01$, and *** = $P < 0.001$. Data are presented as mean + S.E.M., $n = 4$.

ARPE-19 Cells Internalize rhHsp70

The flow cytometry histogram (Fig. 4) shows that both dividing and differentiated ARPE-19 cells internalized rhHsp70. A single peak distinctly shifted to the right represented the positive dataset of dividing ARPE-19 cells (a); whereas flow analysis of differentiated ARPE-19 cells (b) produced a mixed population of cells resulting in two peaks on the histogram. In differentiated ARPE-19 cells, there was no clear separation between cells that had internalized the fluorescent protein (peak on the right) and those that had not (peak overlapping the negative control in grey). The percentage of positive cells,

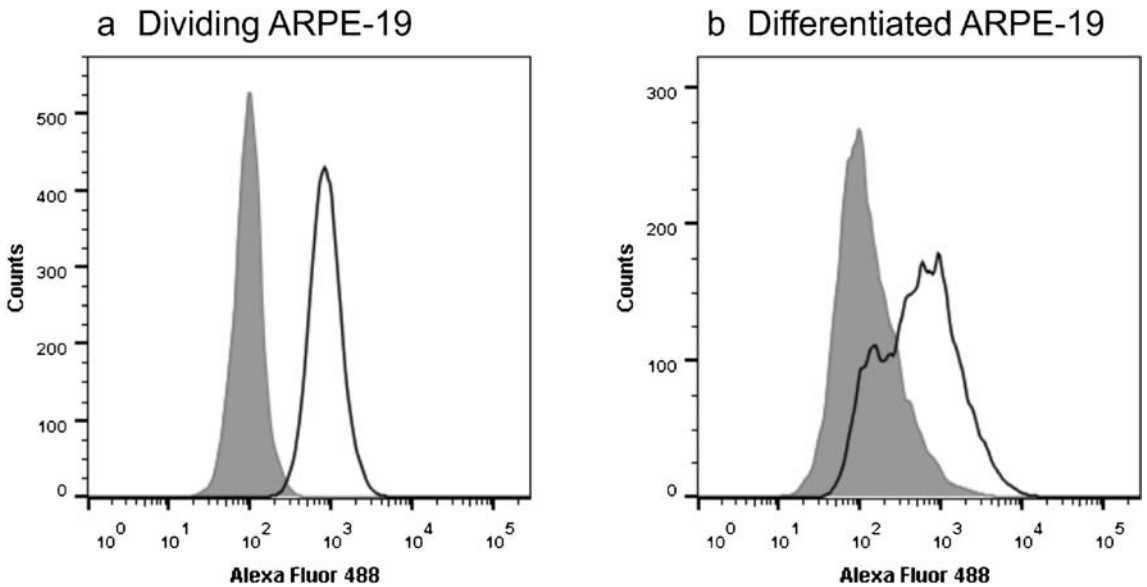

Fig. 4 Internalization of rhHsp70 in ARPE-19 cells. Cell association of rhHsp70 was studied in dividing and differentiated ARPE-19 cells by flow cytometry. (**a**) 97% of dividing ARPE-19 cells was found positive whereas only (**b**) 57% of differentiated ARPE-19 cells had internalized the protein. However, FACS results may underestimate the uptake of differentiated ARPE-19 cells because these cells were found to grow in two layers instead of one (see discussion).

according to the Overton cumulative histogram subtraction algorithm, was 97±2% for dividing ARPE-19 cells and 57± 12% for differentiated ARPE-19 cells.

rhHsp70 is Localized in Lysosomes and Late Endosomes

Intracellular localization of exogenously delivered fluorescently labeled rhHsp70 was studied qualitatively with live cell confocal microscopy (Fig. 5). This method allows distinction between rhHsp70 that is associated with cells and is therefore immobilized on the cell surface, from rhHsp70 that has been internalized and moves intracellularly, *i.e.* together with lysosomes. Endocytosed rhHsp70 (in green) was found in lysosomes and late endosomes (in red) in dividing and differentiated ARPE-19 cells.

rhHsp70 Distributes to the Outer Layers of the eye

Following intravitreal injection into an isolated porcine eye, radiolabeled rhHsp70 diffused from the injection site to the

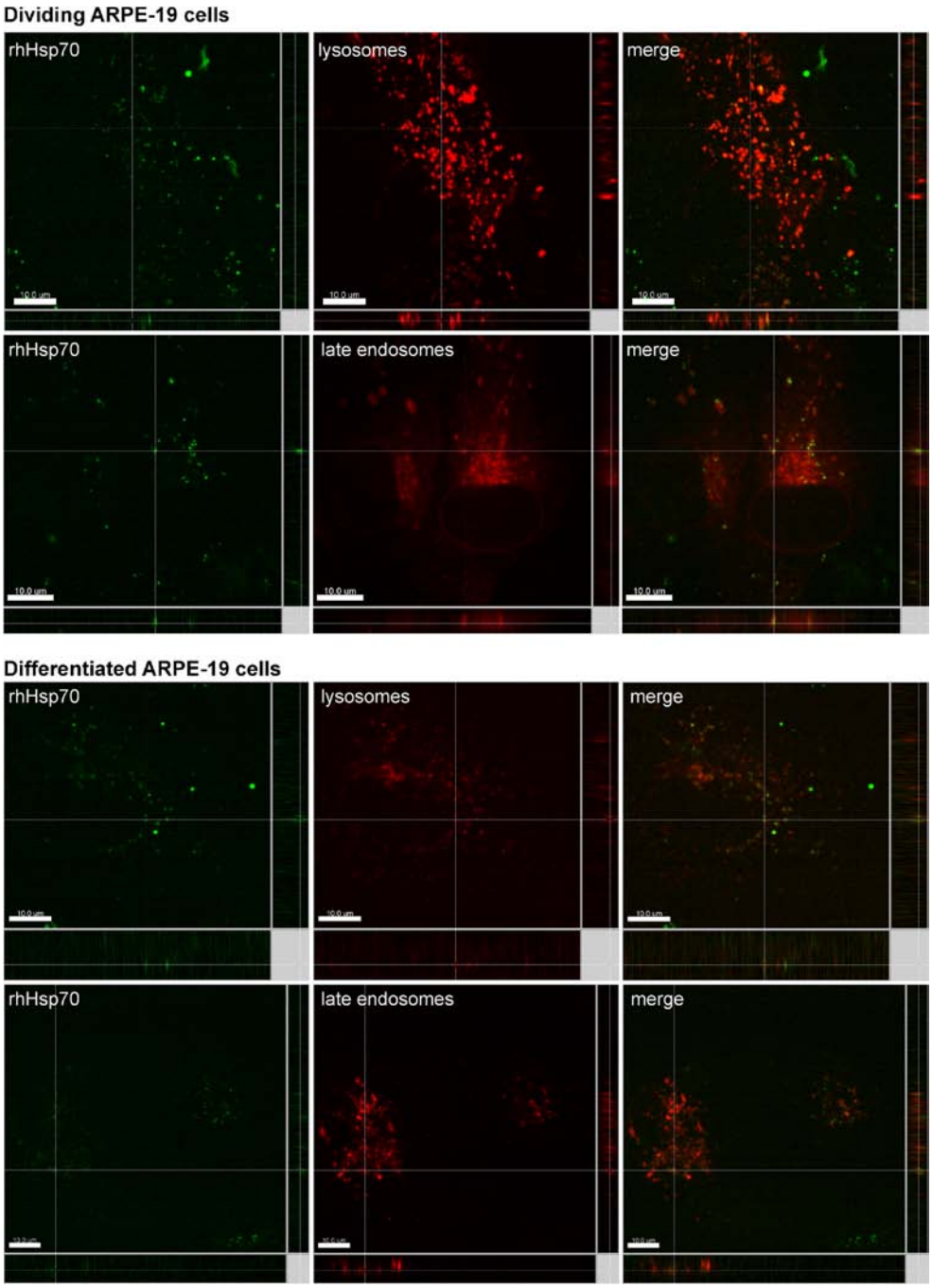

Fig. 5 Intracellular localization of AlexaFluor488 labeled rhHsp70 in living ARPE-19 cells. RhHsp70 (in green) was incubated with the cells for 1 h, immediately thereafter the cells were visualized with a confocal microscope. Lysosomes and late endosomes (in red) were stained with with CellLight RFP reagent. Scale bars are 10 μm.

retina within 30 min (Fig. 6). At 2 h post-injection the protein was still mostly localized in the retina. At later times (4 h and 24 h) rhHsp70 partially diffused back into the vitreous. Even 24 h after administration, the injected protein was not found in the anterior chamber of the eye. In the control eye, radioactive iodide diffused throughout the vitreous, but the signal was lost after 2 h, probably because the radionuclide diffused out of the eye and was diluted in the buffer where eyes were kept between measurements.

The resolution of the micro SPECT/CT instrument was too low to distinguish distribution in the outer tissue layers of the eye; therefore, after the last time point, vitreous, retina, RPE, and sclera were collected and the radioactivity of the single tissues was quantified with a gamma counter. We found 41% of the total collected activity per g tissue in the vitreous, 14% in the retina, 20% in the RPE, and 6% in the sclera.

DISCUSSION

An increasing number of neurodegenerative diseases is characterized by protein misfolding, accumulation of protein aggregates, and abnormal protein degradation. In the case of age-related macular degeneration (AMD), protein aggregates occur both intracellularly inside lysosomes as lipofuscin, and in the form of drusen, in the extracellular space between the RPE and the Bruch's membrane. In healthy RPE cells, detrimental aggregation of proteins is prevented by complex cellular quality control mechanisms; one of these endogenous cytoprotective mechanisms is the heat shock response. Under stress conditions, including oxidative stress, cells respond by activating the synthesis of inducible chaperones called heat shock proteins (Hsps), whose undertakings include the participation in the folding, activation and reactivation of non-native proteins. Hsps are also responsible for facilitating the degradation of proteins that have failed to refold and reactivate, thereby preventing accumulation of protein aggregates and protecting the cells from degeneration. In addition, members of the Hsp70 family, in collaboration with other co-chaperones, have the remarkable function of dissolving protein aggregates (30–32). Clearly, the ability of healthy RPE cells to deal with high levels of oxidative stress is tightly linked to a prompt induction of the heat shock response, which several studies have shown to be dysfunctional in AMD (18–20). Therefore, given the cytoprotective properties of Hsps and their inadequate activation in AMD, rhHsp70 supplementation is a potential therapeutic approach that we wanted to investigate.

To test the efficacy of exogenously delivered rhHsp70 in protecting RPE cells against oxidative stress, we exposed ARPE-19 cells to hydrogen peroxide with and without

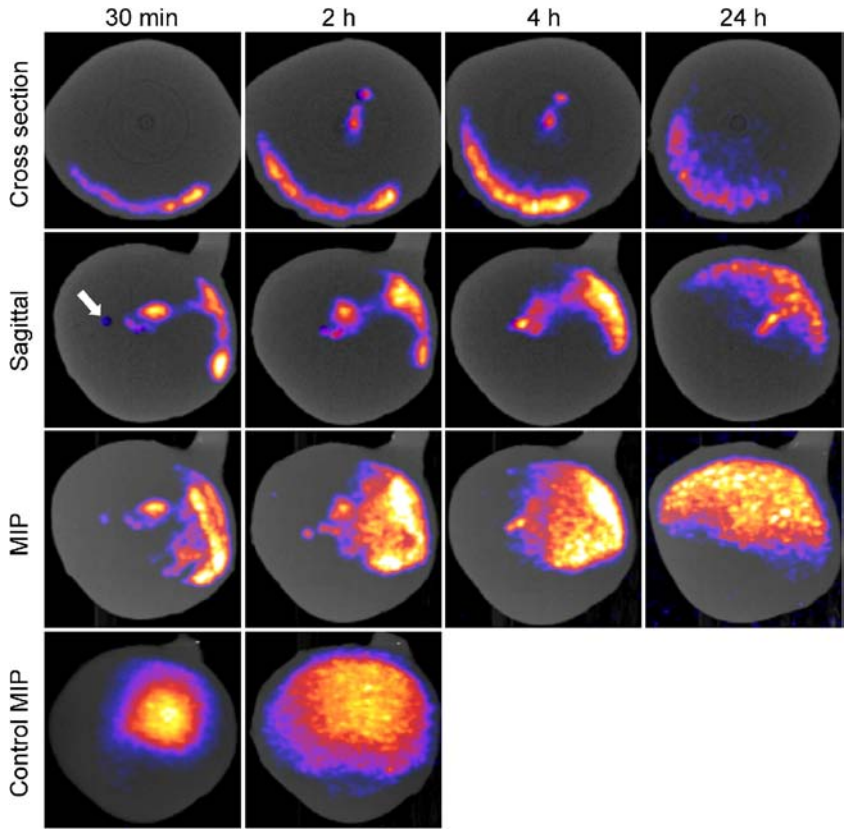

Fig. 6 Intraocular distribution of [^{123}I] rhHsp70 after intravitreal injection (4.4 MBq). Ocular diffusion of [^{123}I] rhHsp70 was followed over a time period of 24 h with micro SPECT/CT. The outer ocular layers were reached within 30 min after administration. The arrow in the sagittal image at 30 min indicates the injection site. MIP: maximum intensity projection.

rhHsp70 pre-treatment. ARPE-19 cells that were pre-treated with rhHsp70 displayed reduced inflammation, higher viability and decreased cytotoxicity compared to cells that did not receive such treatment before the oxidative challenge. The length of rhHsp70 pre-treatment was 24 h, 48 h, or 72 h and was chosen in order to mimic the situation found *in vivo*, indeed the half-life of rhHsp70 in the vitreous is likely to be of several days, similarly to other proteins of comparable size; for example, the intravitreal $t_{1/2}$ of ranibizumab (MW = 48 kDa) is 7.2–9 days (33, 34). The results show that the length of rhHsp70 pre-treatment that we chose for these experiments does not seem to influence the protective effect on ARPE-19 cells. Indeed, in all three assays testing cell health, we found that exogenous delivery of rhHsp70 protected the cells from the oxidative challenge. Our findings are in line with a recently published work (35), which evaluated the antiapoptotic properties of another Hsp, α-crystallin and α-crystallin-derived peptides, in human fetal RPE. Moreover, others and we have previously shown that endogenous Hsp70 is upregulated, promotes cell survival and clearance of lysosomal aggregates after oxidant-mediated injury (8, 21, 22, 25, 30–32). For these reasons we believe that, even if still in its infancy, exogenous delivery of rhHsp70 may be a therapeutic strategy worth pursuing for the treatment of RPE degeneration that is a central hallmark of AMD.

The efficacy of rhHsp70 therapy, however, relies on the successful delivery of the protein to the lysosomes of RPE cells. Therefore, in the second part of our work we concentrated on the feasibility of rhHsp70 protein delivery to the RPE. There are two main aspects to consider when delivering a therapeutic protein to the RPE: firstly, whether the protein is taken up by RPE cells and, if uptake takes place, where is the protein localized intracellularly, and secondly, whether the protein is able to diffuse to the RPE after intravitreal injection. To evaluate the *in vitro* uptake of rhHsp70, we added the fluorescently labelled protein to the culture medium of human retinal pigment epithelial cells (ARPE-19). ARPE-19 cells, when cultured on filters for four weeks, will differentiate into tight cell monolayers mimicking the outer blood-retinal barrier (28). Even though both dividing and differentiated ARPE-19 cells did internalize rhHsp70, only 57% of differentiated ARPE-19 cells were found positive compared to 97% of dividing ARPE-19 cells. A possible explanation to this observation is the fact that differentiated ARPE-19 cells, instead of growing in monolayers, were found to form double layers of cells (confocal microscopy of ARPE-19 cells with labelled cell nuclei, data not shown). We can therefore assume that the upper layer of cells internalized rhHsp70, whereas the lower layer, closer to the filter membrane, could not because it did not have access to the protein. For this reason, we think that the flow cytometry results may underestimate the uptake of labelled rhHsp70 by differentiated ARPE-19 cells. The internalization of a protein in RPE cells is not a trivial problem; in fact a recently published study (35) reported that αB-crystallin, a member of the small heat shock protein (Hsp20) family, did not enter human fetal RPE cells. Our work further showed that exogenously delivered rhHsp70 was localized in late endosomes and lysosomes. Lysosomal targeting of rhHsp70 is a desired feature for rhHsp70 therapy, since it is in the lysosomes that the toxic protein aggregates accumulate and our previous study demonstrated that Hsp70 promoted their clearance (8).

In the ophthalmology practice, therapeutic proteins used in the treatment of wet AMD are administered into the vitreous. For this reason we wanted to evaluate the diffusion of rhHsp70 in the vitreous using the pig eye as an *ex vivo* model. The negatively charged vitreous is a complex three-dimensional network that may restrict the mobility of large cationic molecules (36). Nonetheless, our preliminary study showed that after intravitreal administration radiolabelled rhHsp70 did not remain fixed at the injection site, but instead it rather quickly diffused to the retina and RPE. Hsp70 is negatively charged (pI = 5.48) at physiologic pH, hence electrostatic repulsion may prevent aggregation of the protein in the anionic vitreous humour. From the vitreous rhHsp70 may eventually penetrate the different layers of the retina and reach the RPE *via* passive diffusion. Despite this positive result, we understand that the use of an *ex vivo* model has its shortcomings, the most obvious being the impossibility to evaluate the role of convective flow in the movement of rhHsp70. Furthermore, age-related changes such as vitreous liquefaction and contraction, disease states compromising the tightness of the intraocular barriers, as well as the site of needle placement during injection may also significantly modify the diffusion of rhHsp70 from the site of administration to the retina. Most of the mentioned scenarios however are expected to ease rather than hinder rhHsp70 permeation to the RPE. Nevertheless, the fact that full-sized 150 kDa antibodies are successfully used in the clinical practice to treat retinal neovascularization has established that even large proteins can be targeted to the retina and the RPE after intravitreal injection.

Together our results provide a proof of concept evidence to the applicability of rhHsp70 protein therapy against oxidative stress in AMD as well as the feasibility of rhHsp70 delivery to RPE cells. Future avenues of research should include the formulation of a controlled delivery system that will allow a sustained release of rhHsp70 into the vitreous and consequently decrease the frequency of administration. Several delivery systems have been tested for the controlled release of proteins inside the eye, including implants (Tethadur from pSivida), PLGA microspheres (37–39), nanoparticles (40), and liposomes (41). Another option is encapsulated cell technology; Neurotech's intravitreal implant of encapsulated human retinal pigment epithelial cells releasing ciliary neurotrophic factor (CNTF) (42) is currently in a phase II clinical trial for macular degeneration. Other delivery routes than intravitreal

administration may also be explored, for example computational models have assessed the adequacy of protein delivery through the sclera using hydrogels (43, 44). Moreover protein engineering techniques may enhance rhHsp70 cellular uptake, lysosomal delivery, as well as provide selective targeting to the RPE; therefore increasing the therapeutic efficacy and reducing potential side effects.

CONCLUSION

The treatment of neovascularization in wet AMD has improved enormously since the introduction of anti-neovascular agents; however to date no treatment is available for patients suffering from RPE atrophy. Recently, the chronic exposure to oxidative stress and a decline in lysosomal activity of RPE cells have been recognized as a possible cause for RPE degeneration (2–4). On the contrary to healthy RPE cells, their diseased counterparts are unable to effectively tackle oxidative stress and clear lysosomal aggregates, possibly due to a downregulation of the heat shock response. Our study showed that rhHsp70 therapy to the RPE offered protection against oxidative challenge and that the exogenously delivered protein was internalized into RPE cells and localized inside late endosomes and lysosomes. Furthermore, after intravitreal administration rhHsp70 protein diffused to the outer ocular layers and was found inside the RPE. Overall, this work provides a novel therapeutic option for the treatment of RPE degeneration in AMD.

ACKNOWLEDGMENTS

We would like to thank Ms. Leena Pietilä at the Centre for Drug Research, University of Helsinki and Ms. Anne Seppänen at the Department of Ophthalmology, University of Eastern Finland for technical assistance, the Light Microscopy Unit of the Institute of Biotechnology at the University of Helsinki for help with confocal microscopy, Dr. Mari Raki for operating the micro SPECT/CT, and Dr. Shuang Wang for assistance in image analysis. We also acknowledge the Finnish Funding Agency for Innovation (Tekes), the Friends of the Blind foundation (Sokeain Ystävät ry), Evald and Hilda Nissi foundation, Orion-Farmos research foundation, and Academy of Finland (decision no. 136805) for financial support.

REFERENCES

1. de Jong PTVM. Mechanisms of disease: Age-related macular degeneration. N Engl J Med. 2006;355(14):1474–85.
2. Winkler BS, Boulton ME, Gottsch JD, Sternberg P. Oxidative damage and age-related macular degeneration. Mol Vis. 1999;5 (32–42.
3. Kaarniranta K, Sinha D, Blasiak J, Kauppinen A, Vereb Z, Salminen A, *et al.* Autophagy and heterophagy dysregulation leads to retinal pigment epithelium dysfunction and development of age-related macular degeneration. Autophagy. 2013;9(7):973–84.
4. Jarrett SG, Boulton ME. Consequences of oxidative stress in age-related macular degeneration. Mol Aspects Med. 2012;33(4):399–417.
5. Feeney-Burns L, Hilderbrand ES, Eldridge S. Aging human RPE: morphometric analysis of macular, equatorial, and peripheral cells. Invest Ophthalmol Vis Sci. 1984;25(2):195–200.
6. Sherman MY, Goldberg AL. Cellular defenses against unfolded proteins: A cell biologist thinks about neurodegenerative diseases. Neuron. 2001;29(1):15–32.
7. Calamini B, Morimoto RI. Protein homeostasis as a therapeutic target for diseases of protein conformation. Curr Top Med Chem. 2012;12(22):2623–40.
8. Ryhänen T, Hyttinen JMT, Kopitz J, Rilla K, Kuusisto E, Mannermaa E, *et al.* Crosstalk between Hsp70 molecular chaperone, lysosomes and proteasomes in autophagy-mediated proteolysis in human retinal pigment epithelial cells. J Cell Mol Med. 2009;13(9B):3616–31.
9. Morimoto RI. The heat shock response: systems biology of proteotoxic stress in aging and disease. Cold Spring Harb Symp Quant Biol. 2011;76 (91–99
10. Heydari AR, Takahashi R, Gutsmann A, You S, Richardson A. Hsp70 and aging. Experientia. 1994;50(11–12):1092–8.
11. Locke M, Tanguay RM. Diminished heat shock response in the aged myocardium. Cell Stress Chaperones. 1996;1(4):251–60.
12. Muramatsu T, Hatoko M, Tada H, Shirai T, Ohnishi T. Age-related decrease in the inductability of heat shock protein 72 in normal human skin. Br J Dermatol. 1996;134(6):1035–8.
13. Katayama T, Imaizumi K, Honda A, Yoneda T, Kudo T, Takeda M, *et al.* Disturbed activation of endoplasmic reticulum stress transducers by familial Alzheimer's disease-linked presenilin-1 mutations. J Biol Chem. 2001;276(46):43446–54.
14. Cowan KJ, Diamond MI, Welch WJ. Polyglutamine protein aggregation and toxicity are linked to the cellular stress response. Hum Mol Genet. 2003;12(12):1377–91.
15. Wen FC, Li YH, Tsai HF, Lin CH, Li C, Liu CS, *et al.* Down-regulation of heat shock protein 27 in neuronal cells and non-neuronal cells expressing mutant ataxin-3. FEBS Lett. 2003;546(2–3):307–14.
16. Hay DG, Sathasivam K, Tobaben S, Stahl B, Marber M, Mestril R, *et al.* Progressive decrease in chaperone protein levels in a mouse model of Huntington's disease and induction of stress proteins as a therapeutic approach. Hum Mol Genet. 2004;13(13):1389–405.
17. Zourlidou A, Gidalevitz T, Kristiansen M, Landles C, Woodman B, Wells DJ, *et al.* Hsp27 overexpression in the R6/2 mouse model of Huntington's disease: chronic neurodegeneration does not induce Hsp27 activation. Hum Mol Genet. 2007;16(9):1078–90.
18. Nordgaard CL, Berg KM, Kapphahn R, Reilly C, Feng X, Olsen TW, *et al.* Proteomics of the retinal pigment epithelium reveals altered protein expression at progressive stages of age-related macular degeneration. Invest Ophthalmol Vis Sci. 2006;47(3):815–22.
19. Decanini A, Nordgaard CL, Feng X, Ferrington DA, Olsen TW. Changes in select redox proteins of the retinal pigment epithelium in age-related macular degeneration. Am J Ophthalmol. 2007;143(4):607–15.
20. Nordgaard CL, Karunadharma PP, Feng X, Olsen TW, Ferrington DA. Mitochondrial proteomics of the retinal pigment epithelium at progressive stages of age-related macular degeneration. Invest Ophthalmol Vis Sci. 2008;49(7):2848–55.
21. Strunnikova N, Baffi J, Gonzalez A, Silk W, Cousins SW, Csaky KG. Regulated heat shock protein 27 expression in human retinal pigment epithelium. Invest Ophthalmol Vis Sci. 2001;42(9):2130–8.

22. Strunnikova N, Zhang C, Teichberg D, Cousins SW, Baffi J, Becker KG, *et al.* Survival of retinal pigment epithelium after exposure to prolonged oxidative injury: A detailed gene expression and cellular analysis. Invest Ophthalmol Vis Sci. 2004;45(10):3767–77.
23. Kurz T, Brunk UT. Autophagy of HSP70 and chelation of lysosomal iron in a non-redox-active form. Autophagy. 2009;5(1):93–5.
24. Karlsson M, Frennesson C, Gustafsson T, Brunk UT, Nilsson SEG, Kurz T. Autophagy of iron-binding proteins may contribute to the oxidative stress resistance of ARPE-19 cells. Exp Eye Res. 2013;116 (359–365.
25. Bailey TA, Kanuga N, Romero IA, Greenwood J, Luthert PJ, Cheetham ME. Oxidative stress affects the junctional integrity of retinal pigment epithelial cells. Invest Ophthalmol Vis Sci. 2004;45(2):675–84.
26. Paimela T, Hyttinen JMT, Viiri J, Ryhänen T, Karjalainen RO, Salminen A, *et al.* Celastrol regulates innate immunity response *via* NF-kappa B and Hsp70 in human retinal pigment epithelial cells. Pharmacol Res. 2011;64(5):501–8.
27. Glenn JV, Mahaffy H, Dasari S, Oliver M, Chen M, Boulton ME, *et al.* Proteomic profiling of human retinal pigment epithelium exposed to an advanced glycation-modified substrate. Graefes Arch Clin Exp Ophthalmol. 2012;250(3):349–59.
28. Mannermaa E, Reinisalo M, Ranta VP, Vellonen KS, Kokki H, Saarikko A, *et al.* Filter-cultured ARPE-19 cells as outer blood-retinal barrier model. Eur J Pharm Sci. 2010;40(4):289–96.
29. Hansen MB, Nielsen SE, Berg K. Re-examination and further development of a precise and rapid Dye method for measuring cell-growth cell kill. J Immunol Methods. 1989;119(2):203–10.
30. Glover JR, Lindquist S. Hsp104, Hsp70, and Hsp40: A novel chaperone system that rescues previously aggregated proteins. Cell. 1998;94(1):73–82.
31. Goloubinoff P, Mogk A, Ben Zvi AP, Tomoyasu T, Bukau B. Sequential mechanism of solubilization and refolding of stable protein aggregates by a bichaperone network. Proc Natl Acad Sci U S A. 1999;96(24):13732–7.
32. Mattoo RUH, Sharma SK, Priya S, Finka A, Goloubinoff P. Hsp110 is a bona fide chaperone using ATP to unfold stable misfolded polypeptides and reciprocally collaborate with Hsp70 to solubilize protein aggregates. J Biol Chem. 2013;288(29):21399–411.
33. Krohne TU, Liu ZP, Holz FG, Meyer CH. Intraocular pharmacokinetics of ranibizumab following a single intravitreal injection in humans. Am J Ophthalmol. 2012;154(4):682–6.
34. Xu L, Lu T, Tuomi L, Jumbe N, Lu JF, Eppler S, *et al.* Pharmacokinetics of ranibizumab in patients with neovascular Age-related macular degeneration: a population approach. Invest Ophthalmol Vis Sci. 2013;54(3):1616–24.
35. Sreekumar PG, Chothe P, Sharma KK, Baid R, Kompella U, Spee C, *et al.* Antiapoptotic properties of alpha-crystallin-derived peptide chaperones and characterization of their uptake transporters in human RPE cells. Invest Ophthalmol Vis Sci. 2013;54(4):2787–98.
36. Pitkänen L, Ruponen M, Nieminen J, Urtti A. Vitreous is a barrier in nonviral gene transfer by cationic lipids and polymers. Pharm Res. 2003;20(4):576–83.
37. Jiang C, Moore MJ, Zhang X, Klassen H, Langer R, Young M. Intravitreal injections of GDNF-loaded biodegradable microspheres are neuroprotective in a rat model of glaucoma. Mol Vis. 2007;13(198–99):1783–92.
38. Checa-Casalengua P, Jiang CH, Bravo-Osuna I, Tucker BA, Molina-Martinez IT, Young MJ, *et al.* Retinal ganglion cells survival in a glaucoma model by GDNF/Vit E PLGA microspheres prepared according to a novel microencapsulation procedure. J Control Release. 2011;156(1):92–100.
39. Andrieu-Soler C, Aubert-Pouessel A, Doat M, Picaud S, Halhal M, Simonutti M, Venier-Julienne MC, Benoit JP, Behar-Cohen F. Intravitreous injection of PLGA microspheres encapsulating GDNF promotes the survival of photoreceptors in the rd1/rd1 mouse. Mol Vis. 2005;11 (118–20)
40. Sakai T, Kuno N, Takamatsu F, Kimura E, Kohno H, Okano K, *et al.* Prolonged protective effect of basic fibroblast growth factor-impregnated nanoparticles in royal college of surgeons rats. Invest Ophthalmol Vis Sci. 2007;48(7):3381–7.
41. Abrishami M, Ganavati SZ, Soroush D, Rouhbakhsh M, Jaafari MR, Malaekeh-Nikouei B. Preparation, characterization, and *in vivo* evaluation of nanoliposomes-encapsulated bevacizumab (avastin) for intravitreal administration. Retina-J Ret Vit Dis. 2009;29(5):699–703.
42. Zhang K, Hopkins JJ, Heier JS, Birch DG, Halperin LS, Albini TA, *et al.* Ciliary neurotrophic factor delivered by encapsulated cell intraocular implants for treatment of geographic atrophy in age-related macular degeneration. Proc Natl Acad Sci U S A. 2011;108(15): 6241–5.
43. Ninawe PR, Hatziavramidis D, Parulekar SJ. Delivery of drug macromolecules from thermally responsive gel implants to the posterior eye. Chem Eng Sci. 2010;65(18):5170–7.
44. Kavousanakis ME, Kalogeropoulos NG, Hatziavramidis DT. Computational modeling of drug delivery to the posterior eye. Chem Eng Sci. 2014;108 (203–212.